ESC European Society of Cardiology

Cardiovascular Research (2019) **115**, 357–372
doi:10.1093/cvr/cvy224

Absence of natriuretic peptide clearance receptor attenuates TGF-β1-induced selective atrial fibrosis and atrial fibrillation

Dolkun Rahmutula, Hao Zhang, Emily E. Wilson, and Jeffrey E. Olgin*

Division of Cardiology, Cardiovascular Research Institute, University of California, San Francisco, 505 Parnassus Avenue, M1182, Box 0124, San Francisco, CA 94143, USA

Received 5 November 2017; revised 5 June 2018; editorial decision 25 August 2018; accepted 14 September 2018; online publish-ahead-of-print 18 September 2018

Time for primary review: 35 days

Aims TGF-β1 plays an important role in atrial fibrosis and atrial fibrillation (AF); previous studies have shown that the atria are more susceptible to TGF-β1 mediated fibrosis than the ventricles. Natriuretic peptides (NPs) play an important role in cardiac remodelling and fibrosis, but the role of natriuretic peptide clearance (NPR-C) receptor is largely unknown. We investigated the role of NPR-C in modulating TGF-β1 signalling in the atria.

Methods and results MHC-TGF-β1 transgenic (TGF-β1-Tx) mice, which develop isolated atrial fibrosis and AF, were *cross-bred* with NPR-C knock-out mice (NPR-C-KO). Transverse aortic constriction (TAC) was performed in wild type (Wt) and NPR-C knockout mice to study. Atrial fibrosis and AF inducibility in a pathophysiologic model. Electrophysiology, molecular, and histologic studies were performed in adult mice. siRNA was used to interrogate the interaction between TGF-β1 and NP signalling pathways in isolated atrial and ventricular fibroblasts/myofibroblasts. NPR-C expression level was 17 ± 5.8-fold higher in the atria compared with the ventricle in Wt mice ($P = 0.009$). *Cross-bred* mice demonstrated markedly decreased pSmad2 and collagen expression, atrial fibrosis, and AF compared with TGF-β1-Tx mice with intact NPR-C. There was a marked reduction in atrial fibrosis gene expression and AF inducibility in the NPR-C-KO-TAC mice compared with Wt-TAC. In isolated fibroblasts, knockdown of NPR-C resulted in a marked reduction of pSmad2 (56 ± 4% and 24 ± 14% reduction in atrial and ventricular fibroblasts, respectively) and collagen (76 ± 15% and 35 ± 23% reduction in atrial and ventricular fibroblasts/myofibroblasts, respectively) in response to TGF-β1 stimulation. This effect was reversed by simultaneously knocking down NPR-A but not with simultaneous knock down of PKG-1.

Conclusion The differential response to TGF-β1 stimulated fibrosis between the atria and ventricle are in part mediated by the abundance of NPR-C receptors in the atria.

Keywords Natriuretic peptide receptor • Transforming growth factor-beta1 • Transverse aortic constriction • Cardiac fibrosis • Atrial fibrillation

1. Introduction

Atrial fibrillation (AF) is the most commonly encountered cardiac arrhythmia in clinical practice and is a significant cause of morbidity.[1] AF is associated with increased atrial fibrosis in both humans[2–4] and in multiple animal models of AF.[5–11] We have previously demonstrated an increase in AF vulnerability in a transgenic mouse model overexpressing TGF-β1 (myosin heavy chain promoter driven transgene of constitutively active TGF-β1) with isolated atrial fibrosis.[9,12] In addition, we have previously demonstrated in a canine tachycardia pacing-induced heart failure model, in which atrial fibrosis leads to AF, treatment with the anti-fibrotic agent Pirfenidone reduces TGF-β1 expression, prevents atrial fibrosis, and prevents AF vulnerability.[6] The TGF-β1 pathway appears to be important in human AF as well.[13] Interestingly, in all of the above-mentioned animal models of AF, there is isolated atrial fibrosis. In the ventricular tachycardia pacing-induced heart failure model of AF, there is profound, progressive and irreversible atrial fibrosis, with minimal ventricular fibrosis, and reversible ventricular dysfunction.[10,14] In our TGF-β1 transgenic (TGF-β1-Tx) mouse, there is equal expression of the transgene in the atria and the ventricle, but only fibrosis in the atria.[9,13] Similarly, in humans with

* Corresponding author. Tel: +1 415 476 1325; fax: +1 415 476 9802, E-mail: jeffrey.olgin@ucsf.edu

severe heart failure, there is marked increase in TGF-β1 expression and signalling in the atria (but not ventricle) and atrial fibrosis.[13,15] We sought to determine whether the natriuretic peptide (NP) system may play a role in modulating this differential response to TGF-β1-induced fibrosis.

Atrial natriuretic peptide (ANP), B type natriuretic peptide (BNP), and C type natriuretic peptide[16] have each been shown to antagonize the pro-hypertrophic and pro-fibrotic actions of TGF-β1, AngII, and ET-1 in cardiac myocytes and fibroblasts, either *in vivo* or *in vitro*.[17] It has been also demonstrated that the NP/cGMP/PKG pathway exerts its anti-fibrotic action in isolated cardiac fibroblast by counteracting TGF-β1 signalling.[18] In addition, deletion of the BNP gene[17] or that of its cognate receptor NPR-A in the mouse heart is associated with increased interstitial fibrosis.[19] ANP can inhibit the renin-angiotensin system, prevents fibrosis, and suppresses TGF-β1 expression,[20] and BNP has been shown to antagonize TGF-β-dependent pro-fibrotic activity in cultured cardiac fibroblasts.[21] The majority of NP signalling in the heart is thought to occur via the NPR-A receptor, which is relatively abundant in both the atria and ventricle; however, the natriuretic peptide clearance (NPR-C) receptor, which functions predominantly as a clearance receptor[22] has markedly different expression patterns in the atria compared with the ventricle. At the cellular level, NP receptors have been previously shown to be expressed in ventricular myocytes and ventricular fibroblasts, but have not been well studied in atrial fibroblasts.[23,24] In this study, we tested the hypothesis that the differential expression of the NPR-C in the atria and the ventricle, in part contribute to the differential response to TGF-β1 stimulation between atria and ventricles. Furthermore, we hypothesize that knocking out NPR-C will protect the atria from TGF-β1-induced fibrosis and AF.

2. Methods

The data, analytic methods, and study materials will be/have been made available to other researchers for purposes of reproducing the results or replicating the procedure upon request.

2.1 Animals

All studies were approved and monitored by the UCSF Laboratory Animal Resource Center and conformed to the 'Guide for the Care and Use of Laboratory Animals' (National Institutes of Health publication, 8th Edition, 2011). MHC-TGFcys33ser (TGF-β1-Tx)[9,12,13] and NPR-C-KO[25] mice were generated and bred as previously described. *Cross-bred* were made by crossing TGF-β1-Tx$^{+/-}$ with NPR-C$^{-/-}$ mice. Offspring underwent genotyping using PCR of DNA isolated from tail biopsies. The following groups of littermate mice (F2) were studied in a blinded fashion: (i) wild type (Wt), (ii) Tx, (iii) NPR-C$^{-/-}$, (iv) Tx$^{+/+}$/NPR-C$^{+/-}$, and (v) Tx$^{+/+}$/NPR-C$^{-/-}$. A transverse aortic constriction (TAC) model of the left ventricular overload made on Wt and NPR-C$^{-/-}$ mice (age of 9–12 weeks) using a minimally invasive transverse aortic binding technique. After anaesthetized by inhalation of 1.5% isoflurane of oxygen with a face mask, the mice were placed supine and body temperature is maintained at 37°C on a heating pad. Buprenorphine (60 μg/kg) and ketoprofen (5 mg/kg) are given subcutaneously 10 min prior to surgery.[26,27] For both electrophysiology studies and molecular experiments, 16 weeks of age, mice were studied.

2.2 Tissue histology

Histology and fibrosis quantification was performed as previously described.[9] Whole hearts were sectioned, fixed, and stained with Sirius red/fast green. Fibrosis was quantified by measuring red pixel content of digitized photomicrographs relative to total tissue area.

2.3 Mouse echocardiography

Both control and TAC mice were examined by non-invasive transthoracic echocardiography during baseline and 8 weeks post-TAC surgery using previously described methods.[28] Two-dimensional echocardiography was performed using a high-resolution echocardiography system (Vevo 770, VisualSonics, Toronto, Canada), equipped with a 30 MHz transducer. LV interventricular septal thicknesses, LV internal dimensions, and posterior wall thicknesses at diastole and systole were measured at the level of the papillary muscles to determine the left ventricular end-systolic and end-diastolic volumes, left ventricular ejection fraction (EF), and fractional shortening.

2.4 Mouse electrophysiology studies

2.4.1 Optical mapping

Optical mapping was performed on Langendorff perfused hearts using a 100 × 100 CMOS camera (Ultima, SciMedia) within a 5 × 5 mm mapping field focused on the atria, as previously described.[9,29] Mice were injected with heparin (10 U/g) and euthanized with Urethane (2 g/kg). The heart was rapidly excised and harvested in cold cardioplegia solution. The aorta was cannulated and perfused at a pressure of 80 mmHg with modified Krebs–Henseleit solution. Pacing electrodes were sutured to each of the right atrium and left atrium. The cannulated heart was then placed in 37°C Tyrode solution in a temperature-controlled optical recording chamber (maintained at 37°C). The hearts were perfused with Tyrode solution containing the voltage-sensitive dye di-4-ANEPPS (10 μL of 2.5 mM stock). Contractility was blocked using 5 μM blebbistatin.

Optical maps were acquired at 1000 Hz during programmed electrical stimulation and were recorded during pacing drives of 150, 120, 90, 80, and 60 ms. The effective refractory period (ERP) was determined in the left atria (LA) and right atria (RA) during S1–S2 pacing with a basic (S1) pacing cycle length (PCL) of 100 ms for 2 s, followed by a single extrastimulus (S2), progressively decremented by 2 ms intervals from 50 ms until loss of capture. AF inducibility was further tested by burst pacing for 2 s, with a cycle length ranging from 40 to 20 ms with a 2 ms decrement. AF was defined as a period of rapid irregular atrial rhythm lasting at least 2 s. Optical mapping data was analysed as previous described[13,30,31] using OMproCCD software (courtesy of Bum-rak Choi, Providence, RI, USA) and custom developed analyses software using MatLab. Isochronal activation maps, conduction velocity (using velocity vectors), and conduction heterogeneity were analysed as described previously.[5,13,32] For conduction heterogeneity, phase differences were calculated as average differences with neighbouring activation times at each site. Frequency histograms were then constructed for phase differences within a recorded area. These histograms were summarized as phase time at the 5th (P5), 50th (P50), and 95th percentiles (P95) of the distribution. To quantify conduction heterogeneity, we calculated the conduction heterogeneity index, defined as (P95-P5)/P50.[33] The action potential duration (APD) at 80% repolarization (APD_{80}) was measured for each of the optical action potential.

2.4.2 Transoesophageal electrophysiological study

AF inducibility studies on intact animals were performed in control and TAC mice as previously described.[13] For these studies, transoesophageal electrophysiology studies (using a 4 Fr quadripolar catheter)[13] in anaesthetized mice were performed to allow sequential comparison before and after TAC. Mice were anaesthetized and surface (standard limb leads), and oesophageal ECGs were recorded. Inducibility of atrial arrhythmias was tested by transoesophageal burst pacing to capture the

atria (but not ventricle), for 2 s, with a cycle length ranging from 40 to 20 ms with a 2 ms decrement. AF was defined as a period of rapid irregular atrial rhythm lasting at least 2 s.

2.5 Molecular studies

The mice were injected with heparin (10 U/g) and euthanized with Urethane (2 g/kg) intraperitoneal (IP) injection and the heart was removed. Protein and RNA were isolated separately from the atria and the ventricles from 10 mice in each group above. Total protein (30 mg) was electrophoresed on 4–12% Tris-Glycine-polyacrylamide gels and transferred onto polyvinylidene difluoride membrane. Membranes were incubated with rabbit polyclonal antibody against the proteins shown in Supplementary material online, *Table S1*. Mouse monoclonal anti-GAPDH antibody at 1:5000 dilutions was used to detect GAPDH as a loading control. Membranes were then incubated with horseradish peroxidase-conjugated goat anti-mouse antibody or goat anti-rabbit antibody for 1 h, and then washed with Tris-buffered saline/Tween. Blots were immersed for 2 min in enhanced chemiluminescence detection reagent, exposed to film and quantified by densitometry (standardized to the GAPDH band). Antibodies directed against Smad2/3, phospho-Smad2, and secondary antibody goat anti-rabbit were purchased from Millipore (MA, USA). Anti-PKG-1 antibody and anti-TGF-β1 antibody were from Cell Signaling Inc. (MA, USA). Anti-GAPDH and secondary antibody goat anti-mouse were purchased from Santa Cruz Biotechnology (CA, USA).

Total RNA isolated from mice were analysed by qRT-PCR. A 1 μg of RNA was used to reverse transcribe cDNA (Clontech, CA, USA). The targeting genes (Supplementary material online, *Table S2*) and GAPDH were synthesized by Applied Biosystems (CA, USA). Real-time PCR was performed using Taqman master mix (Applied Biosystems, Inc.) with an ABI 7300 (Applied Biosystems, Inc.). Negative controls without input cDNA were used to assess signal specificity. All gene transcript levels were quantified and normalized for GAPDH transcript levels in each sample. Equivalent amounts (0.5 μL) of cDNA were used for measurement of targeting genes and GAPDH gene transcripts. All samples were amplified in triplicate. Relative quantification was achieved by the comparative $2^{-\Delta\Delta Ct}$ method.[34] The relative increase/decrease (fold-induction/repression) of mRNA of target *x* in the experimental group was calculated using the control group as the calibrator 2^{-Ct}, where cycle threshold (C_t) are: $\{C_{t.x}[Tx] - C_{t.GAPDH}[Tx]\} - \{C_{t.x}[Wt] - C_{t.GAPDH}[Wt]\}$, $\{C_{t.x}[Wt\text{-}TAC] - C_{t.GAPDH}[Wt\text{-}TAC]\} - \{C_{t.x}[Wt] - C_{t.GAPDH}[Wt]\}$, $\{C_{t.x}[NPR\text{-}C\text{-}KO\text{-}TAC] - C_{t.GAPDH}[NPR\text{-}C\text{-}KO\text{-}TAC]\} - \{C_{t.x}[NPR\text{-}C\text{-}KO] - C_{t.GAPDH}[NPR\text{-}C\text{-}KO]\}$ and $\{C_{t.x}[A\text{-}Fibs] - C_{t.GAPDH}[A\text{-}Fibs]\} - \{C_{t.x}[V\text{-}Fibs] - C_{t.GAPDH}[V\text{-}Fibs]\}$.

2.6 cGMP measurements in tissue

For cGMP measurements, hearts from each group ($n = 5$) were weighed and homogenized in 10 volumes of cold 5% trichloroacetic acid using a polytron homogenizer. Samples were centrifuged at 1500×*g* for 10 min and the supernatants were then extracted using water-saturated ether. cGMP was measured in acetylated supernatants using an EIA kit, according to the manufacturer's instruction (Cayman Chemical). cGMP content is expressed as pmol/mL wet tissue.

2.7 Studies in isolated fibroblasts

In order to further interrogate molecular pathways involved in NPR-C regulation of TGF-β1-induced fibrosis, isolated fibroblasts were used. Specific parts of the NP signalling pathway were modified using siRNA and cells were exposed to TGF-β1 with a readout of pSmad-2 and collagen production. The mice were injected with heparin (10 U/g) and euthanized with urethane (2 g/kg) IP injection and the heart was removed. Fibroblasts were separately isolated from atria and ventricles of adult mouse hearts and liver with digestion PBS buffer (containing 1 mg Collagenase B, 1 mg Trypsin, and 0.015 mg DNAase in 1 mL PBS). All tissues were kept on ice and washed with PBS more than three times, then minced into 2–3 mm sized pieces. Minced tissues were digested at 37°C for 10 min, and then washed with 10 mL of foetal bovine serum (FBS). After tissue was fully digested by repeating this procedure, the suspension was filtered with a 50 μm strainer. The filtered suspension was then spun at 1200 rpm for 5 min and the pellet was placed in Dulbecco's modified Eagle's medium (DMEM) H-21 supplemented with 5–20% FBS. Cells were then incubating at 37°C for 24 h prior to exposure to TGF-β or siRNA. Fibroblasts were maintained in serum-free media (DMEM) H-21 for 72 h prior to experiments. All experiments were performed with primary cultured cells.

For experiments involving knocking down RNA, cells were treated for 48 h with 45 pmol/mL siRNA (Supplementary material online, *Table S3* and *Figure S3*). Serum-starved cells were exposed to 5 ng/mL rhTGF-β1 (R&D, MN, USA) for 24 h following the siRNA treatment. Cells were then lysed (1 × RIPA buffer for protein and using Qiagen RNeasy Mini Kit for RNA isolation) for immunoblotting and qRT-PCR, as described above. All RNA knock-downs were confirmed using qRT-PCR and immunoblotting.

2.8 Statistical analysis

One-way ANOVA with Tukey's multiple comparisons test and *t*-test were used to assess significance for continuous variables. The proportion of mice with AF inducibility was analysed using the Pearson χ^2 among groups.

3. Results

3.1 Mouse histology studies

Cardiac histology demonstrated the expected increase in atrial fibrosis without any increase in ventricular fibrosis in TGF-β1-Tx mice compared with Wt (*Figure 1A*), as previously reported.[9,12,13] The ventricle in all of the mouse models and intercrosses showed no morphologic abnormalities and demonstrated no increase in fibrosis compared with Wt. Consistent with the collagen expression data (see below), there was no significant increase in fibrosis in the atria or ventricles of the NPR-C-KO mice. In addition, the TGF-β1-Tx/NPR-C-KOh and TGF-β1-Tx/C-KO intercrosses demonstrated an attenuation of atrial fibrosis compared with TGF-β1-Tx mice (*Figure 1A* and *B*). Sirius red/fast green staining of sections from post-TAC hearts revealed a greater degree of chamber enlargement and fibrosis in Wt when compared with NPR-C-KO mice, particularly in the LA and LV (Supplementary material online, *Figure S4*). The α-SMA staining of sections from post-TAC hearts shown much higher expression level of α-SMA in Wt-TAC-LA compare to all other sections (Supplementary material online, *Figure S4*). In western blot, the α-SMA protein expression level is less in NPR-C-KO-TAC-LA compared with Wt-TAC-LA, but this was not statistically significant compared with NPR-C-KO-LA (*Figure 5*).

3.2 Comparison of cardiac function between Wt and NPR-C-KO mice after TAC

There was no differences in cardiac function or size between NPR-C-KO and Wt without TAC. Likewise, there were no differences in cardiac

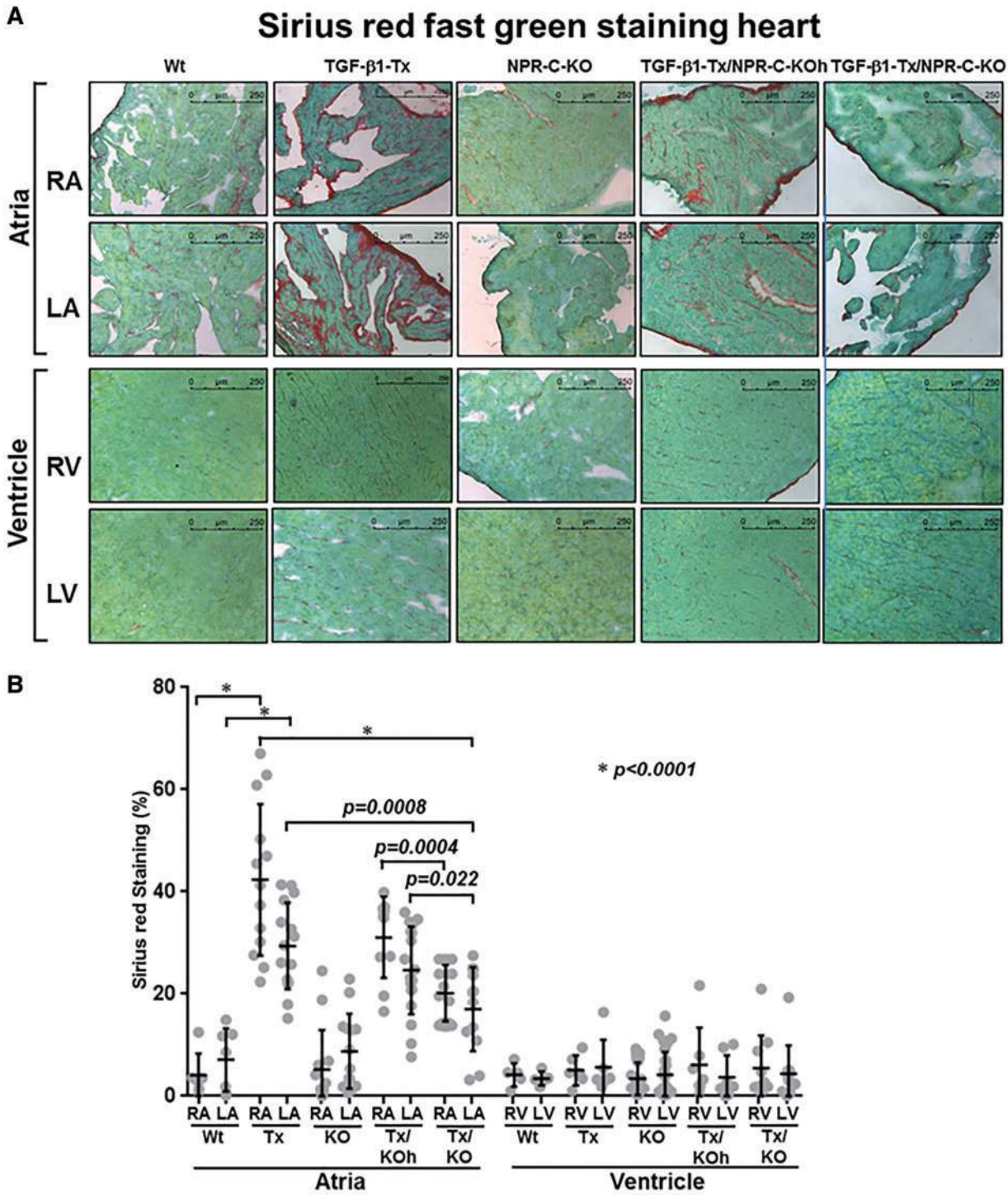

Figure 1 Histology of Wt and the TGF-β1-Tx, NPR-C knockout, and TGF-β1-Tx cross NPR-C-KO model. (*A*) Sirius red/fast green staining of both atria and ventricle from Wt ($n = 10$), TGF-β1-Tx ($n = 10$), NPR-C ($n = 10$), and TGF-β1-Tx/NPR-C-KO ($n = 10$) mice. Magnified view of atria (upper panel) and ventricle (lower panel), photomicrographic magnifications are ×200. (*B*) Quantification of fibrosis, one-way ANOVA Tukey's multiple comparisons test used to produce the *P* values.

function or size between TGF-β1-Tx or intercrosses. Both Wt and NPR-C-KO mice developed heart failure 8 weeks post-TAC surgery. There was no difference in EF at baseline between Wt-TAC and NPR-C-KO-TAC groups (EF: 71.5 ± 3.4% vs. 81.0 ± 2.23%). The EF was significantly decreased after TAC (EF: 71.5 ± 3.4% vs. 39.17 ± 4.6% in Wt group, and 81.0 ± 2.23% vs. 49.55 ± 5.06% in NPR-C-KO group, $P < 0.01$) and there was no significant difference in the EF between Wt and NPR-C-KO group after TAC (*Figure 2A*, Supplementary material online, *Figure S4E* and *Table S4*).[35]

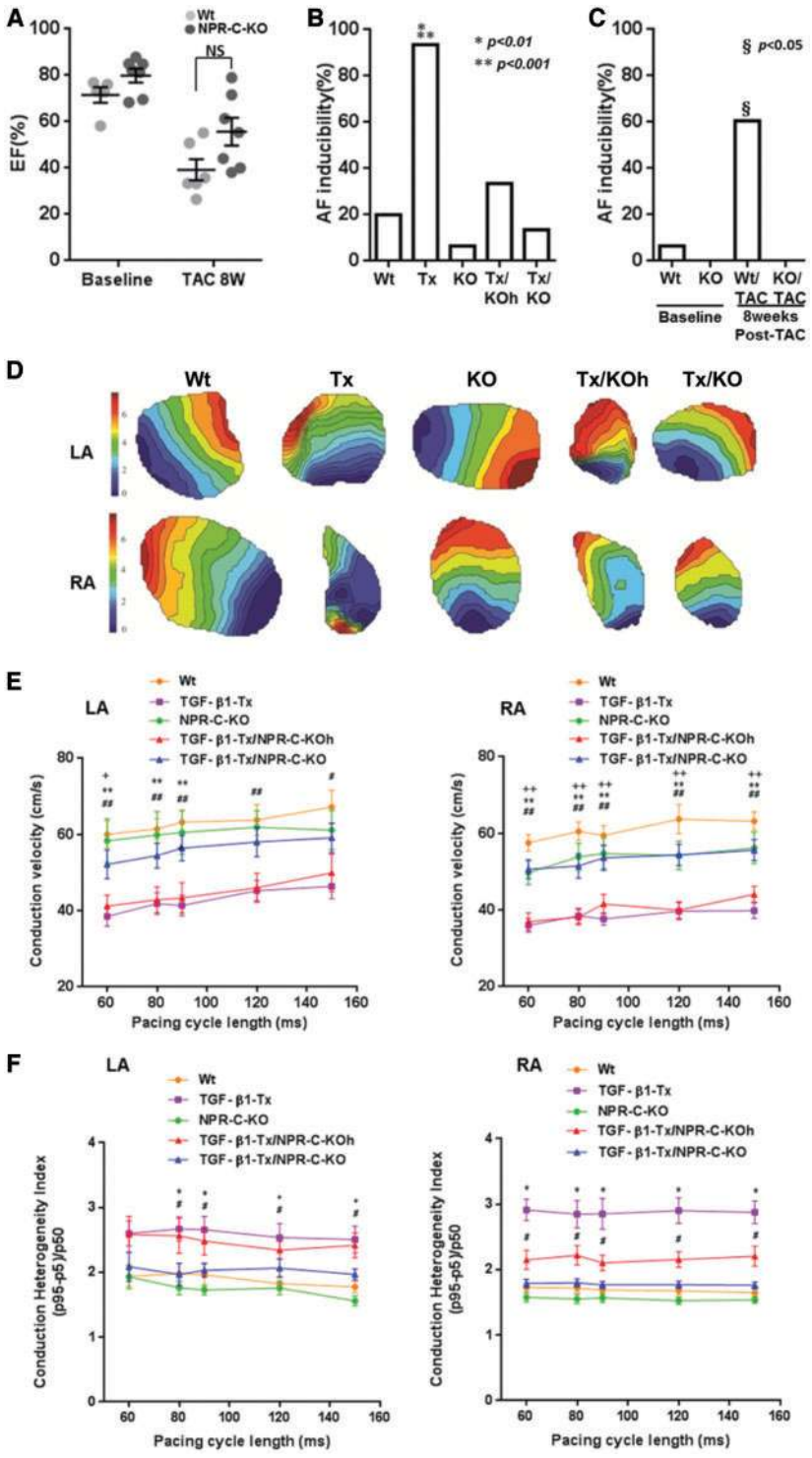

Figure 2 Echocardiography and electrophysiologic properties. (*A*) Left ventricular EF determined by echocardiography of Wt ($n = 10$) and NPR-C-KO ($n = 10$) mice at baseline (before TAC) and 8 weeks after TAC. (*B*) AF inducibility in *cross-bred* mice among groups of the Wt ($n = 15$), Tx ($n = 15$), KO ($n = 15$) mice, Tx/KOh mice ($n = 15$), and Tx/KO mice ($n = 15$). Wt, wild type; Tx, TGF-β1 transgenic; KO, NPR-$C^{-/-}$ knock out; Tx-KOh, TGF-$\beta1^{+/+}$ transgenic with NPR-$C^{+/-}$ heterozygous knockout; Tx-KO, TGF-$\beta1^{+/+}$ transgenic with NPR-$C^{-/-}$ homozygous knockout. (*C*) AF inducibility of Wt ($n = 15$) and NPR-C-KO ($n = 10$) mice at baseline and 8 weeks post-TAC. Lower number of total mice at 8 weeks reflects mortality from TAC surgery in each group. $^{\S}P < 0.05$ compared with NPR-C-KO mice in TAC groups. AF, atrial fibrillation; TAC, transverse aortic constriction. (*D*) Representative isochronal activation maps of LA and RA from different groups. The isochronic maps of the RA and LA from TGF-β1-Tx mice and LA from TGF-β1-Tx/NPR-C-KOh mice show crowding and heterogeneous conduction pattern compared with those from other mice. (*E*) Conduction velocity of LA and RA from different groups. $^{+}P < 0.05$, *Tx/NPR-C-KO* vs. *TGF-β1-Tx/NPR-C-KOh*, *TGF-β1-Tx*; $n = 15$. $^{**}P < 0.01$, *NPR-C-KO* vs. *TGF-β1-Tx/NPR-C-KOh*, *TGF-β1-Tx*; $^{\#}P < 0.05$, *TGF-β1-Tx* vs. *Wt*. $^{\#\#}P < 0.01$, *Wt* vs. *TGF-β1-Tx/NPR-C-KOh*, *TGF-β1-Tx*; $^{++}P < 0.01$ *TGF-β1-Tx/NPR-C-KO* vs. *TGF-β1-Tx/NPR-C-KOh*, *TGF-β1-Tx*. (*F*) Conduction heterogeneity index of LA and RA from different groups. $^{*}P < 0.05$, *TGF-β1-Tx* vs. *TGF-β1-Tx/NPR-C-KO*, *NPR-C-KO*, and *Wt*; $^{\#}P < 0.05$, *TGF-β1-Tx/NPR-C-KOh* vs. *NPR-C-KO*; $^{+}P < 0.05$, *NPR-C-KO* vs. *TGF-β1-Tx*; one-way ANOVA Tukey's multiple comparisons test used to produce the *P* values and the proportion of mice with AF inducibility was analysed using the Pearson χ^2 among groups.

3.3 Mouse electrophysiology studies

Similar to our previous studies, AF inducibility was significantly higher in TGF-β1-Tx mice compared with Wt control mice (93.3% vs. 20%, $P < 0.001$) as shown in *Figure 2B*. NPR-C-KO mice had no increased vulnerability to AF (6.7%) compared with Wt (20%, P = NS). *Cross-bred* mice in which NPR-C was knocked out in one (TGF-β1-Tx/NPR-C-KOh) or both (TGF-β1-Tx/NPR-C-KO) alleles had reduced AF inducibility (33.3% and 13.3%, respectively) compared with TGF-β1-Tx mice with intact NPR-C genes (93.3%, $P < 0.0001$), as shown in *Figure 2B*.

Conduction velocities determined by optical mapping were lower in both the LA and RA of TGF-β1-Tx mice compared with Wt control mice at all PCL ($P < 0.01$), as shown in *Figure 2D* and *E*. NPR-C-KO mice had similar conduction velocities to that of Wt control mice at all PCLs (P = NS). In the *cross-bred* mice, knocking out one NPR-C allele (TGF-β1-Tx/NPR-C-KOh), did not have a significant effect of conduction velocity compared with TGF-β1-Tx mice at any PCL (P = NS) as shown in *Figure 2E*. However, *cross-bred* mice with the TGF-β1 transgene and both NPR-C alleles knocked out (TGF-β1-Tx/NPR-C-KO), had conduction velocities similar to Wt and NPR-C-KO (without TGF-β1 transgene) mice (P = NS).

Conduction heterogeneity, a marker of AF substrate as previously reported,[9] was significantly increased in Tx mice compared with Wt at all PCLs ($P < 0.05$), as shown in *Figure 2F*. Conduction heterogeneity was similar in NPR-C-KO mice compared with Wt (P = NS). Decreased or elimination of NPR-C appeared to improve the increased conduction heterogeneity in those mice with the TGF-β1 transgene in a dose dependent fashion (*Figure 2D* and *F*). TGF-β1-Tx/NPR-C-KO with both NPR-C alleles knocked out had conduction heterogeneities similar to those mice without the TGF-β1 transgene (Wt and NPR-C-KO) across all pacing rates. TGF-β1-Tx/NPR-C-KOh with a single NPR-C allele knocked out had conduction velocities intermediate between TGF-β1-Tx and Wt mice across all paced rates.

There were no differences in ERP amongst any of the mouse models in the right atrium (Supplementary material online, *Figure S1A*). However, in the LA, the ERP of all the models with NPR-C knocked out (NPR-C-KO = 34.00 ± 5.61, TGF-β1-Tx/NPR-C-KOh = 33.16 ± 7.55, and TGF-β1-Tx/NPR-C-KO = 35.50 ± 7.06) had ERPs that were similar and were significantly longer than Wt (24.5 ± 8.72) and TGF-β1-Tx (27.87 ± 4.50) ($P < 0.01$ and $P < 0.05$, respectively). APDs (APD10, APD50, and APD80) and dF/dt were not different when compared within LA or RA among the five groups (showing in Supplementary material online, *Figure S1A–D*).

3.4 AF inducibility in mice after TAC

To determine whether modulation of fibrosis by NPR-C-KO identified in our transgenic mouse module can be reproduced in a pathophysiologic model of AF vulnerability, we studied AF inducibility before and 8 weeks after TAC. AF inducibility was significantly higher in the Wt group than in NPR-C-KO group 8 weeks after TAC (60% vs. 0%, $P < 0.05$) (*Figure 2C*). There was no difference in AF inducibility between Wt and NPR-C-KO group at baseline prior to TAC.

3.5 Mouse molecular studies

3.5.1 Absent NPR-C increasing activation of NPs and prevent TGF-*β*1-induced cardiac fibrosis

mRNA levels of the NP receptors were vastly different in the atria compared with the ventricle (*Figure 3*). NPR-A expression was two-fold higher in the Wt-Atria compared with Wt-Ventricle. NPR-B expression was 1.5-fold higher in the Wt-Atria compared with Wt-Ventricle. NPR-C expression was more than 40-fold higher in the Wt-Atria compared with the ventricle. None of the receptor expression was significantly altered in the ventricle of the TGF-β1-Tx mice. However, NPR-A and NPR-B expression was increased, whereas NPR-C was decreased in the atria of TGF-β1-Tx mice. Even with the decrease, NPR-C remained more than 20-fold higher in the TGF-β1-Tx atria compared with TGF-β1-Tx ventricle. As expected, the NPR-C-KO mice had very low levels of NPR-C detected by qRT-PRC and no change in the other receptors. Western blots confirmed these differences in NPR-C expression at the protein level (*Figure 4*).

Expression of the three different NPs are shown in *Figure 3*. In general, all NP's mRNA are expressed in higher levels in the atria than the ventricle and the NPR-C-KO mice have a marked increase in ANP and BNP mRNA expression in the atria compared with the ventricle. ANP and BNP mRNA were somewhat increased in TGF-β1-TxA compared with Wt-Atria. There was an increase in cGMP level in the atria of those mice without NPR-C compared with those with NPR-C (Supplementary material online, *Figure S2*), demonstrating increased NPR-A signalling in those mice. PDE5A mRNA was significantly increased in TGF-β1-Tx atria compared with Wt, but there were no differences in PDE5A mRNA in the ventricle amongst the groups. TGF-β1 overexpression increased PDE5A mRNA in the atria regardless of the presence of NPR-C (*Figure 3*).

As expected, collagen-1 and Lox mRNA expression were increased in the TGF-β1-TxA compared with WtA and to TxV (*Figure 3*). The NPR-C-KO mice had no difference in mRNA expression of collagen-1 or Lox in the atria or ventricle compared with Wt (*Figure 3*). The intercross of TGF-β1/Tx and NPR-C-KO demonstrated a decrease in collagen-1 mRNA expression in the atria of those mice heterozygous for the NPR-C deletion (TGF-β1-Tx/NPR-C-KOh) and a further reduction in those mice homozygous for the NPR-C deletion (TGF-β1-Tx/NPR-C-KO) compared with the TGF-β1-TxA, as shown in *Figure 3*. There were no differences in collagen-1 or Lox mRNA in the ventricle amongst any of the mice (*Figure 3* and Supplementary material online, *Figure S5*). Protein levels of collagen-1 paralleled findings from mRNA analyses, with marked increase in collagen-1 protein in TGF-β1-TxA and an attenuation of this increase in the TGF-β1-Tx/NPR-C-KOh and TGF-β1-Tx/NPR-C-KO mice (*Figure 4*). A similar pattern is seen with levels of pSmad2, a pivotal signalling step for the canonical TGF-β1 pathway (*Figure 4*); pSmad2 is increased in the TGF-β1-TxA, but not in TGF-β1-TxV. NPR-C-KO mice have no increase in pSmad2 in either the atria or ventricle. The intercross of TGF-β1-Tx and NPR-C-KO mice yields an attenuation of pSmad2 in the atria, with a decrease in the TGF-β1-Tx/NPR-C-KOh mice and further decrease in the TGF-β1-Tx/NPR-C-KO mice compared with the TGF-β1-TxA (*Figure 4*), There were no changes to the TGF-β receptors TGFβR-I and TGFβR-II in the ventricle between any of the models. TGFβR-I was increased in the atria of TGF-β1 overexpressing transgenic mouse model, but this increase was attenuated with heterozygous and homozygous deletion of NPR-C in a step-wise fashion in the *cross-bred* models. There was no significant differences in TGFβR-II expression amongst any of the models. All of this molecular data demonstrates an attenuation of TGF-β1 signalling in those transgenic intercross mice not expressing NPR-C. There were no differences in overall Smad2/3 expression in the atria in any of the mouse models (*Figure 4*). As expected, all mice overexpressing TGF-β1 had a decrease in the inhibitory Smad7 in the atria but not in the ventricle (*Figure 4*).

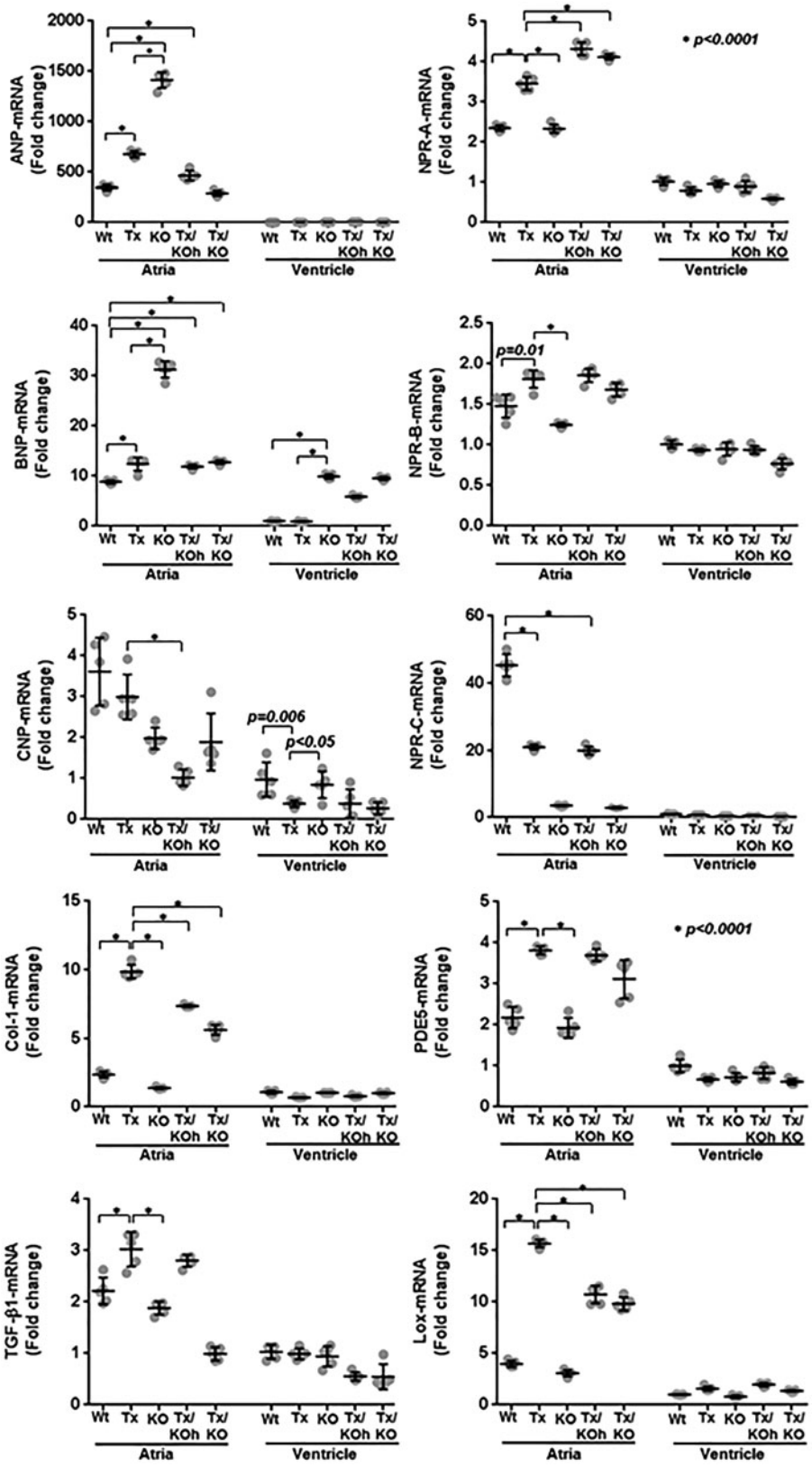

Figure 3 mRNA expression level of natriuretic peptides, receptors, and fibrosis-related genes in murine atrial and ventricular tissue. mRNA was measured from Wt, Tx, NPR-C-KO, and Tx *cross-bred* with NPR-C knockout (TGF-β1-Tx/NPR-C-KO) were determined by qRT-PCR isolated from both atrial and ventricular tissues of mouse heart in each of five different groups of mice. $n = 5$; one-way ANOVA Tukey's multiple comparisons test used to produce the *P* values.

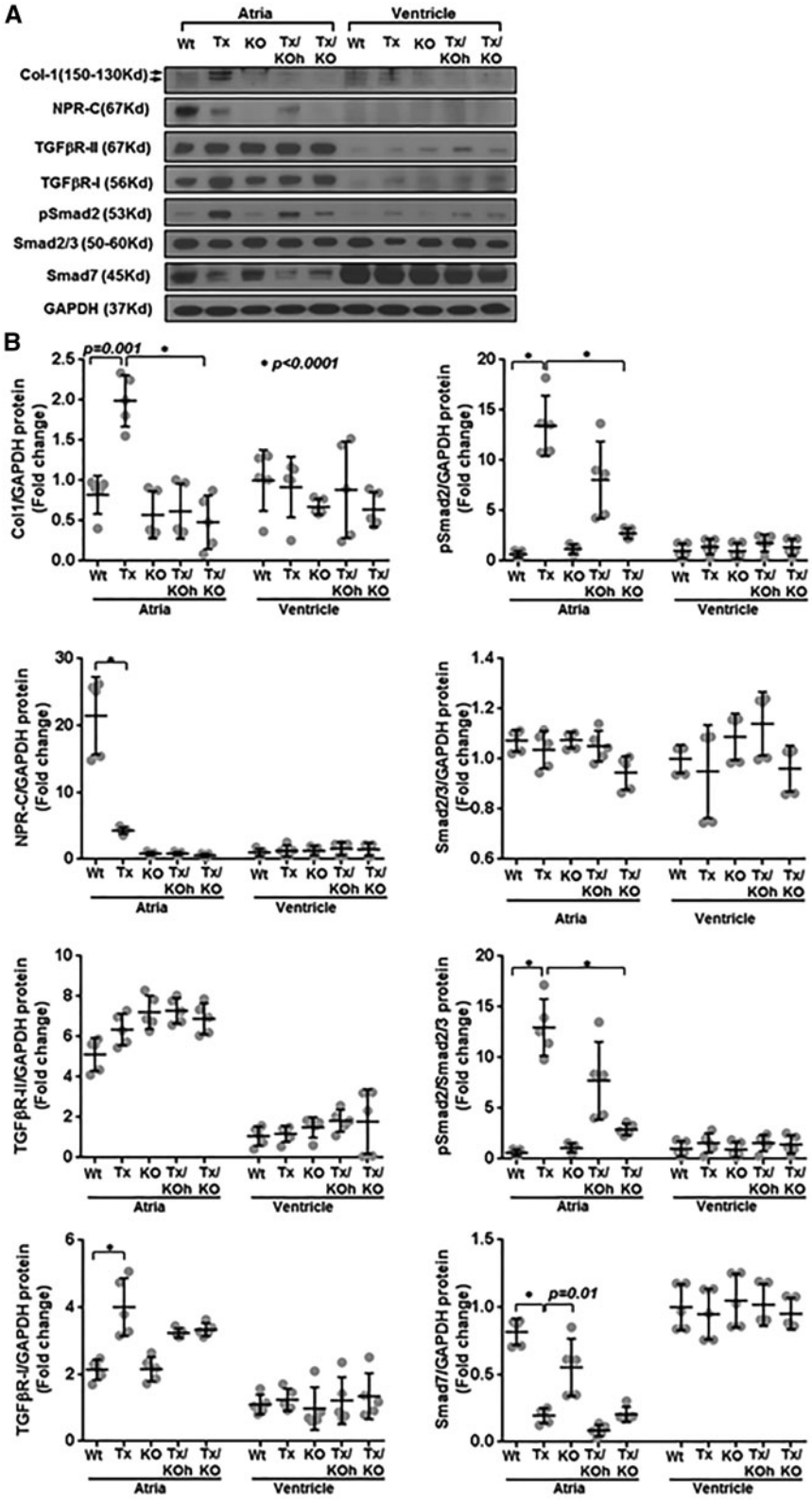

Figure 4 Fibrosis-related protein levels in atrial and ventricular tissue of *cross-bred* mice. Wt, Tx, NPR-C-KO, and Tx cross NPR-C-KO were determined by western blot. (*A*) Western blot analysis with anti-Col-1, anti-NPR-C, anti-pSmad2, anti-Smad2/3, anti-Smad7, and anti-GAPDH in both atrial and ventricular tissues of mouse heart with five different groups of mice. (*B*) Pooled data from five independent western blot analyses (all results normalized for GAPDH). Wt, wild type; Tx, TGF-β1 transgenic; KO, NPR-$C^{-/-}$ knock out; Tx-KOh, TGF-$\beta1^{+/+}$ transgenic with NPR-$C^{+/-}$ heterozygous knockout; Tx-KO, TGF-$\beta1^{+/+}$ transgenic with NPR-$C^{-/-}$ homozygous knockout; one-way ANOVA Tukey's multiple comparisons test used to produce the *P* values.

3.5.2 NPR-C knockout blunts TGF-β1 signalling and atria fibrosis in TAC model

Similar to our findings in our TGF-β1-Tx mice, downstream TGF-β1 signalling and fibrosis were inhibited by absence of NPR-C in TAC mice. As expected, NPR-C was absent in the ventricle of both Wt and NRP-C-KO-TAC mice and the atria of NPR-C-KO -TAC mice. The protein expression level of FN1, Periostin, α-SMA, and pSmad2

increased much less in NPR-C-KO-TAC than Wt-TAC-LA (*Figure 5B* and *C*), and Collagen-1 showed a smaller increase at both the mRNA and protein level compare to Wt-TAC-LA (*Figure 5A*). Interestingly, NPR-A was decreased at the mRNA level in both RV and LV of Wt-TAC compared with Wt control, whereas it increased in the LV of NPR-C-KO-TAC vs. NPR-C-KO without TAC. Moreover, BNP mRNA level also increased dramatically in both RV and LV of NPR-C-KO-TAC, but only LV of Wt-TAC increased significantly compared with Wt. Another interesting finding is that mRNA level of NPR-C is significantly elevated in both RV and LV of Wt-TAC mice (ventricular comparison data showing in Supplementary material online, *Figure S6*).

3.6 Isolated fibroblasts studies

3.6.1 siRNA-NPR-C knockdown prevents TGF-β1-induced fibrotic changes of cardiac fibroblasts/myofibroblasts

To further identify the mechanism of NPR-C modulation on TGF-β1-induced fibrosis and to better characterize differences in cardiac fibroblasts from the atria and ventricle, isolated fibroblasts/myofibroblasts were studied. As can be seen in *Figure 6*, mRNA of NPR-A and NPR-C are expressed 3.49-fold and 3.48-fold higher in atrial fibroblasts/myofibroblasts compared with ventricular fibroblasts/myofibroblasts, respectively ($P < 0.0001$). This is also seen at the protein level, where NPR-C protein is 16-fold higher in isolated atrial fibroblasts/myofibroblasts compared with isolated ventricular fibroblasts/myofibroblasts or liver fibroblasts/myofibroblasts used as a non-cardiac control (*Figure 7*). To further compare, the differential response of atrial and ventricular fibroblasts/myofibroblasts to TGF-β1 stimulation, we determined the protein expression level of FN1, Periostin and α-SMA. Both FN1 and Periostin are significantly higher in atrial fibroblasts vs. ventricular fibroblasts/myofibroblasts. α-SMA is higher in atrial fibroblasts/myofibroblasts, but not statistically significant (*Figure 7*). Knocking down NPR-C with siRNA, dramatically blunted the TGF-β1 induced increase in pSmad2 and Collagen-1 effect (*Figure 8*) in either atria or ventricular fibroblasts/myofibroblasts (*Figures 6* and *8*).

3.6.2 NPR-C and TGF-β1 crosstalk differences in atrial-ventricular fibroblast/myofibroblasts occurs indirectly through NPR-A signalling

Knocking down NPR-A with siRNA, resulted in an increase in pSmad2 without TGF-β1 stimulation and an exaggerated response to TGF-β1 stimulation in both atrial and ventricular fibroblasts/myofibroblasts (*Figure 8*), though the responses were more dramatic in the atrial fibroblasts/myofibroblasts. Likewise, knocking down NPR-A resulted in an increase in collagen-1 production with and without TGF-β1 stimulation in both the atrial and ventricular fibroblasts/myofibroblasts (*Figure 8*). In order to determine whether the modulation of TGF-β1 signalling by NPR-C occurred directly through NPR-C or indirectly via NPR-A/PKG-1 (by decreasing NP clearing and thus more availability for NPR-A inhibition of TGF-β1 signalling), we simultaneously knocked out both NPR-C and PKG-1 or NPR-C and NPR-A in cardiac fibroblasts isolated from mouse atria and ventricle (*Figure 8A–D*). When PKG-1 was knocked down, pSmad2 increased and increased significantly more than normal fibroblasts when the cells were stimulated with TGF-β1 (*Figure 8A* and *B*). In addition, when PKG-1 and NPR-C were simultaneously knocked down there was no increase in pSmad2 at baseline and the pSmad2 increased in response to TGF-β1 stimulation, was significantly blunted. Effects on Collagen-I protein were similar and paralleled that of pSmad2 (*Figure 8*). However, when NPR-C and NPR-A was simultaneously knocked down, the antifibrotic effects of NPR-C knock-down was eliminated as demonstrated by enhanced Col-1 and pSmad2 production in response to TGFβ-1 stimulation (*Figure 8A* and *B*). In other words, the blunting effect of knocking down NPR-C on TGF-β1 stimulation of pSmad production was eliminated when NPR-A was simultaneously knocked down (*Figure 8*), but not when PKG-1 was knocked down. These findings occurred in both atrial fibroblasts/myofibroblasts and ventricular fibroblasts/myofibroblasts, but were more pronounced in the atrial fibroblasts/myofibroblasts (*Figure 8C* and *D*).

4. Discussion

The major findings from our study include: (i) NPR-C expression levels are significantly higher in atrial tissues and atrial fibroblasts/myofibroblasts compared with the ventricle and ventricular fibroblasts/myofibroblasts; (ii) absence of NPR-C reduces TGF-β1-induced atrial fibrosis (and prevents the resultant substrate for AF) in two mouse models (TGF-β1-Tx and in a TAC model) as well as TGF-β1 signalling and collagen production in atrial fibroblasts/myofibroblasts; (iii) the mechanism by which NPR-C appears to 'enhance' atrial response to TGF-β1 occurs via suppression of NPR-A/cGMP signalling since simultaneously knocking down NPR-A eliminated the inhibitory effect of knocking down NPR-C on TGF-β1 signalling; and (iv) the selective atrial fibrosis that occurs with TGF-β1 exposure either in our mouse models or in isolated fibroblasts/myofibroblasts may in part be accounted for by the dramatically higher levels of NPR-C present in atria (and atrial fibroblasts/myofibroblasts) which, at least in part, blunts the antifibrotic effects of NPR-A activation.

4.1 The significance of absent NPR-C in preventing atrial fibrosis and AF

Interestingly, investigators have shown that human fibroblasts from different sites of skin displayed distinct and characteristic transcriptional patterns.[36] Previous studies have demonstrated the atria are more susceptible to fibrosis than that the ventricle. In models of reversible heart failure produced by tachy-pacing, the atria become profoundly fibrotic and have a vulnerable substrate to AF[5,6]; moreover, there is minimal ventricular fibrosis,[10] and when the pacing is stopped, the LV function returns to normal, yet atrial fibrosis, and fibrillation remain.[37] Other animal models of AF which mimic disease conditions predisposing to AF show similar patterns of isolated atrial fibrosis such as the ovine chronic HTN model[7]; an ovine obesity model,[8] and a rat obstructive sleep apnoea model.[38] Moreover, our transgenic mouse model, which overexpresses TGF-β1 at similar levels in the atria and ventricle (via a MHC-driven promoter) produces isolated atrial fibrosis and AF.[13] Accornero *et al.*[39] demonstrated similar results—increased fibrotic changes in the atria compared with the ventricle—in an inducible TGF-β1-overexpression model. Moreover, there is evidence that fibroblasts from atria are phenotypically different than those from the ventricle.[11,13] Our previous studies in tissues from humans with heart failure suggest that TGF-β1 is important in human AF and that heart failure patients have a selective increase in atrial TGF-β1, paralleling findings in multiple animal studies.[13]

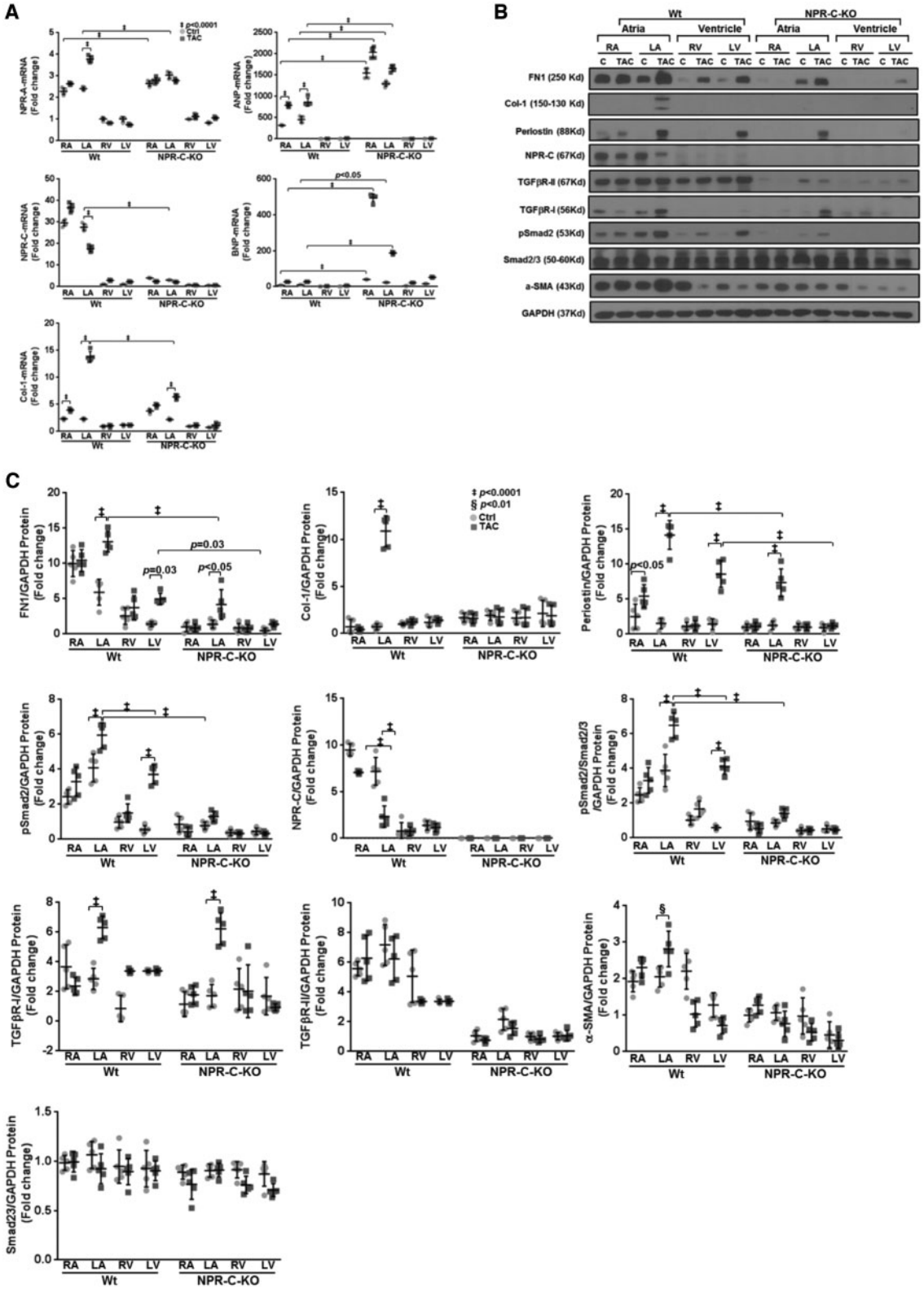

Figure 5 mRNA and protein levels of natriuretic peptides, receptors, and fibrosis-related genes in atrial and ventricular tissue of TAC mice. Wt, Wt-TAC, NPR-C-KO, and NPR-C-KO-TAC were determined by qRT-PCR. (*A*) The mRNA expression levels of natriuretic peptide system and Collagen-1 in both atrial and ventricular tissues of mouse heart with five different groups of mice are shown. (*B*) Wt, Wt-TAC, NPR-C-KO, and NPR-C-KO-TAC were determined by western blot. western blot analysis with anti-FN1, anti-Col-1, anti-Periostin, anti-NPR-C, anti-TGFβR-I, anti-TGFβR-II, anti-pSmad2, anti-Smad2/3, anti-α-SMA, and anti-GAPDH in both atrial and ventricular tissues of mouse heart with five different groups of mice. C, control; TAC, transverse aortic constriction. (*C*) Summary data from western blot analyses using densitometry (all results normalized for GAPDH). $n = 5$; one-way ANOVA Tukey's multiple comparisons test used to produce the *P* values.

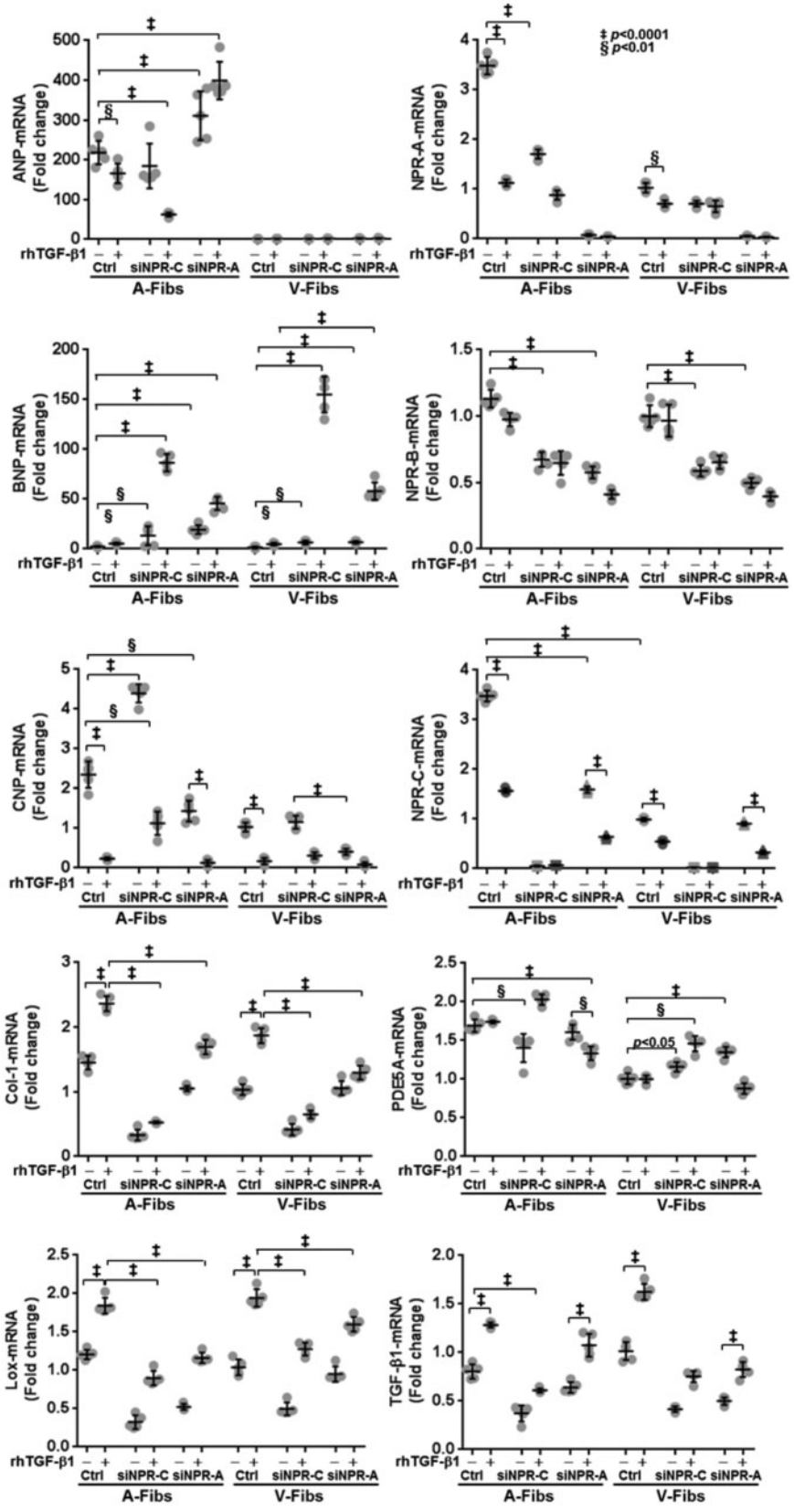

Figure 6 mRNA levels of natriuretic peptides, receptors, and fibrosis-related genes in response to rhTGF-β1 stimulation and NP receptor knockdown in isolated atrial and ventricular fibroblasts/myofibroblasts. qRT-PCR analysis of mRNA levels normalized to GAPDH in the absence or in the presence of an siRNA sequence specific for NPR-A and NPR-C of NP system genes and fibrosis-related genes. rh, recombinant human. $n = 5$; one-way ANOVA Tukey's multiple comparisons test used to produce the *P* values.

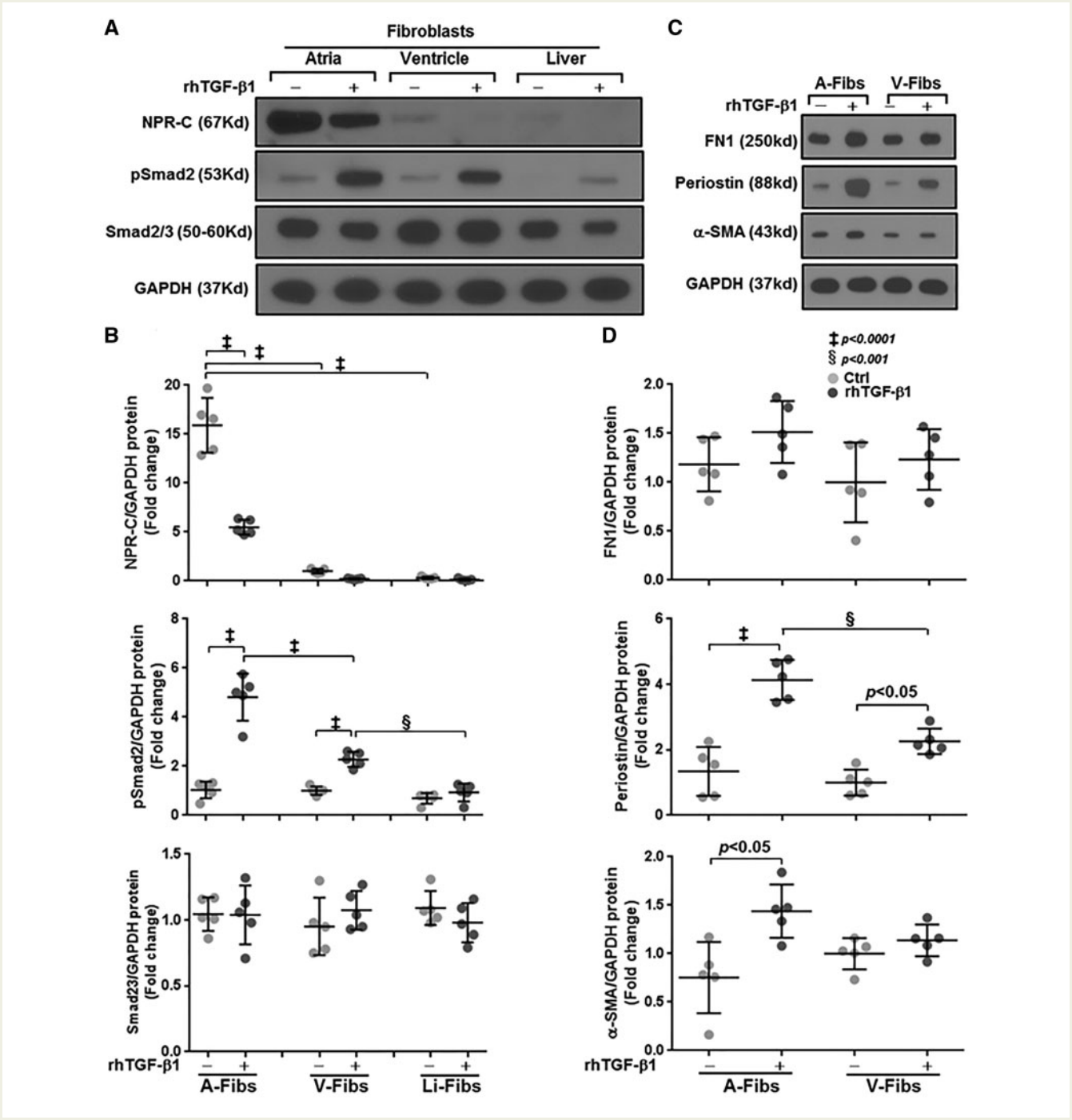

Figure 7 Protein levels of NPR-C in atrial, ventricular, and liver fibroblasts/myofibroblasts in response to TGF-β1 stimulation. Cardiac and liver fibroblasts were maintained in serum-free media for 18 h before treatment with vehicle or rhTGF-β1 (2.5 ng/mL). (*A*) Western blot analysis with anti-NPR-C, anti-pSmad2, and anti-GAPDH. (*B*) Summary data from western blot analyses using densitometry (all results normalized for GAPDH). $n = 5$. rh, recombinant human. (*C*) Western blot analysis with anti-FN1, anti-Periostin, anti-α-SMA, and anti-GAPDH. (*D*) Summary data from western blot analyses using densitometry (all results normalized for GAPDH) $n = 5$. rh, recombinant human; one-way ANOVA Tukey's multiple comparisons test used to produce the *P* values.

The current study further demonstrates physiologic and molecular differences between atrial fibroblasts/myofibroblasts and ventricular fibroblasts/myofibroblasts. Our data suggests that the abundance of NPR-C in the atria and atrial fibroblasts may contribute to this differential response in atrial (compared with ventricular) fibrosis. The low abundance of NPR-C in the ventricle does not mean it is completely resistant to fibrosis; clearly ventricular fibrosis occurs under many circumstances. However, an abundance of NPR-C in the atria appears to make it more susceptible to fibrosis and may explain the heightened fibrotic response seen in several animal models.[5,7–10,13,38]

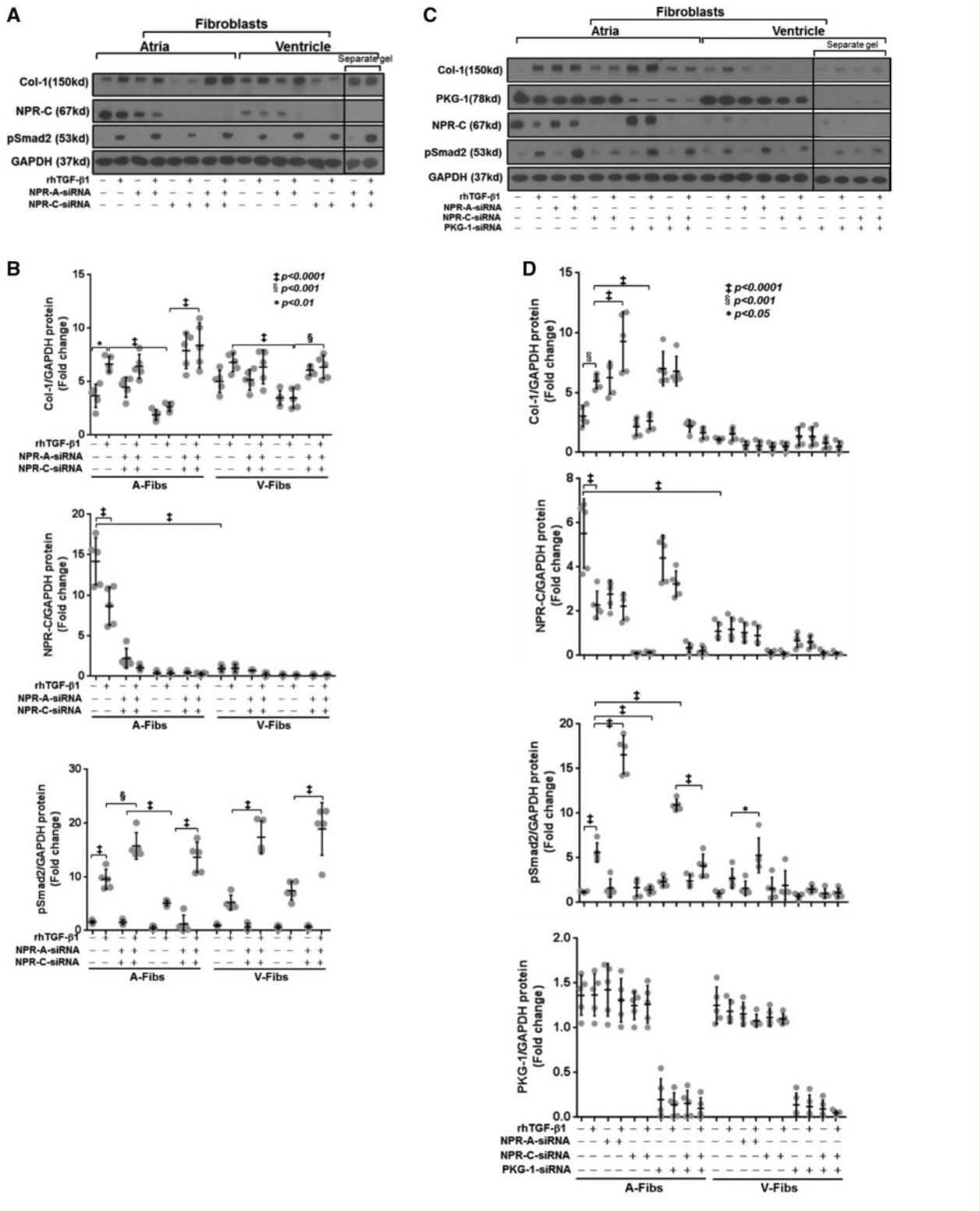

Figure 8 Effect of simultaneous knock down of NPR-C with NPR-A or PKG-1 on TGF-β1 signalling in isolated atrial and ventricular fibroblasts/myofibroblasts. Cardiac fibroblasts/myofibroblasts were maintained in serum-free media for 18 h before treatment with vehicle or siRNA (45 pmol/mL) or rhTGF-β1 (2.5 ng/mL). (*A*) Western blots of Collagen 1 and pSmad2 and (*B*) Summary quantification from densitometry (normalized to GAPDH) of experiments with siRNA to knockdown NPR-C and NPR-A. (*C*) Western blots of Collagen 1 and pSmad2 and (*D*) Summary quantification from densitometry (normalized to GAPDH) of experiments with siRNA to knockdown NPR-C and PKG-1 simultaneously. $n = 5$; one-way ANOVA Tukey's multiple comparisons test used to produce the *P* values.

NPR-C is commonly thought of as a clearance receptor and is widely distributed in many tissues and cell types.[23] It plays an important role in controlling local effects of the NP system.[25] Though some have proposed that the NPR-C may provide some direct signalling function,[40] our data suggest that the effect of NPR-C on modulating TGF-β1 signalling and fibrosis occurs indirectly via NPR-A signalling, with corresponding increase in cGMP and elimination of the anti-fibrotic effects of knocking down NPR-C when NPR-A is also knocked down. This suggests that knocking out NPR-C likely increases local NPs concentration and inhibition of TGF-β1 pro-fibrotic pathways.

We further confirmed the role of NPs in inhibition of TGF-β1 signalling and anti-fibrotic effects in atrial remodelling due to heart failure from TAC in mice. In our study, both Wt and NPR-C-KO mice developed HF as shown by echocardiography. Similar to previous reports, we have demonstrated that atrial fibrosis and enhanced AF inducibility occurs in a pathophysiologic model.[41] When TAC was performed in NPR-C-KO mice, there was a marked decrease in atrial fibrosis and AF inducibility, confirming that a similar signalling process occurs in a pathophysiologically relevant model.

It is also plausible that increases in local NPs may have an effect on atrial myocyte electrophysiology. Others have reported increases in conduction velocity and changes in refractoriness with exogenous ANP. Both Crozier *et al.* and Stambler *et al.*[42–44] reported that acutely-administered exogenous ANP decreased conduction velocity and ERP, the latter study demonstrating that these effects may be mediated via the autonomic nervous system. Yoshida *et al.*[44] demonstrated that this effect on ERP was blunted in animals that had undergone remodelling. Our study shows that when NPR-C is knocked out, APD is unchanged, but atrial ERP is somewhat prolonged compared with Wt mice in a Langendorff preparation (in which there is no effect of autonomics).[45] Our optical mapping study in isolated mouse hearts showed the beneficial effect of knocked-off NPR-C on AF inducibility in TGF-β1-Tx mice. In addition, we showed that knocking out NPR-C affected atrial electrophysiology, such as prolonging ERP and improved conduction velocity and conduction heterogeneity in TGF-β1-Tx mice. These changes result in decreased AF vulnerability.[9] Although a recent study[46] found a modest increased susceptibility to AF in mice lacking NPR-C receptor, this difference may be due to the heart preparation during optical mapping. We performed optical mapping in the intact heart using a Langendorff-perfused preparation. The results from our study showed that atrial conduction velocities in NP-RC-KO mouse hearts were 40–65 cm/s, which was more consistent with other reports in either intact isolated hearts[47,48] or *in vivo* animals.[49] We found similar results in a pathophysiologic model of AF using TAC knocking out NPR-C prevented the development of a vulnerable substrate for AF. Our findings are somewhat at odds with a recent study by Egom *et al.*[46] which found a modestly increased susceptibility to AF in mice lacking NPR-C. However, there are several important differences in that study and the one reported herein. Our study was aimed at the mechanism by which NPR-C might affect fibrosis in models that promote fibrosis, while the Egom study focused primarily on sinus node function and did not study the effects of NPR-C on modulating remodelling and fibrosis. Our findings are not only based on the results from isolated hearts using two different models of atrial fibrosis and AF, but supported by molecular studies in isolated fibroblasts. There were also some important methodological differences; optical mapping performed by Egom *et al.* utilized a cut-open superfused preparation (which may produce some ischaemia in thicker parts of the atria), while we performed optical mapping in the intact heart using a Langendorff-perfused preparation. This can significantly affect electrophysiology parameters and arrhythmia inducibility. It is conceivable that some of the anti-fibrillatory effects observed in our study were due in part to the lengthening of refractoriness (in this case, post-repolarization refractoriness); nonetheless, in addition to these findings there was profound modulation of fibrosis and TGF-β1 signalling in our TGF-β1-Tx model of AF.

The role of the NP system in human AF is not clear. Increased serum BNP has been associated with AF.[50–52] However, this may simply reflect the underlying pathophysiology of heart failure or increased wall stretch, rather than a reflection of the local paracrine milieu. AF is associated with atrial depletion of ANP and low atrial ANP levels have been associated with recurrent AF and increased atrial fibrosis.[53] A frameshift mutation in ANP has been demonstrated to cause familial AF in one family.[54] While this mutant ANP appears to cause a decrease in atrial APD,[54] others have found that this mutant ANP also slows conduction and is pro-fibrillatory, whereas wild-type ANP was shown to be protective.[55] Genetic variants of ANP have also been reported to be associated with AF in a Chinese population,[56] though the precise mechanism is not clear. In all of these circumstances, the effects of the NP system on fibrosis has been implicated as a possible mechanism.

4.2 The mechanism of NPs modulation of cardiac fibrosis

NPs have been identified previously in cardiac fibroblasts and postulated to play an important role in the regulation of TGF-β1 gene signalling activity and fibrosis. NPs possess anti-proliferative activity in cultured cardiac fibroblasts.[24,57,58] However, the mechanism(s) underlying this anti-proliferative activity is not well understood. TGF-β1 is a well described activator of fibroblasts proliferation and pro-fibrotic activity in the heart.[59] BNP has been shown to suppress TGF-β1 activity at multiple loci in cultured cardiac fibroblasts,[21] with demonstrated antagonism at the level of genes involved in fibrosis. Li *et al.*[18] demonstrated that ANP prevents TGF-β-dependent phosphorylation of Smad3, thereby preventing Smad3 nuclear translocation and activation of downstream TGF-β activity. Our data suggests that the effect may also occur more proximal in the TGF-β1 signalling cascade, since we also demonstrated decrease in pSmad2 with knockout of NPR-C. This effect was reversed when NPR-A was simultaneously knocked down; however, not when PKG-1 was simultaneously knocked down, suggesting it may occur via PKG-1-independent signalling.

We have also demonstrated a positive feedback loop between TGF-β1 signalling and NPR-C expression. TGF-β1 appears to suppress NPR-C expression in our transgenic mice overexpression TGF-β1; however, NPR-C levels in the atria in these mice are still quite high. A similar pattern is seen in isolated atrial fibroblasts—TGF-β1 stimulation results in a decrease of NPR-C expression but not to a level where that decrease effects NP suppression of the pro-fibrotic response. One mechanism by which the changes in NPR-C transcript levels may occur has been suggested by the studies of Currie *et al.*[60,61] Using ligand-receptor binding methods, they have demonstrated the preferential down regulation of NPR-C in cultured endothelial cells exposed to high ANP concentration and have reproduced the phenomenon by increasing intracellular GMP with 8-bromo-cGMP and the cGMP phosphodiesterase inhibitor, M&B 22948.[60] In addition, in cultured vascular smooth muscle cells NPR-C was down-regulated by elevating cGMP with sodium nitroprusside and by manoeuvers that induce nitric oxide synthesis.[61] Thus down-regulation of NPR-C in fibrotic cardiac tissue may be mediated by changes in intracellular cyclic GMP as a consequence of

up-regulation of NPR-A which occurs contemporaneously. These findings also support our findings of NP/cGMP suppression of TGF-β1 signalling and regulation of NPR-C expression in the heart.

4.3 Significance

To our knowledge, this is the first demonstration of a critical role for NPR-C in the regulation of TGF-β1 signalling in the cardiac fibroblasts/myofibroblasts proliferation, atrial fibrosis and AF. Our findings also have important therapeutic implication. Identifying targets to prevent or reverse fibrosis would likely be a promising approach to preventing and treating AF.[62] Targeting NPR-C may be an interesting target that might confer relative selectivity to the atria, given the dramatically higher expression level in the atria. There is considerable interest in the pharmacological use of NPR-C specific ligands to reduce NP clearance, and thus enhance their actions.

4.4 Study limitations

All of our cellular work was performed in first-passage cultured cardiac fibroblasts/myofibroblasts. However, there is a possibility that fibroblasts/myofibroblasts were contaminated with a small number of other cells; however, this would likely be a very small number given the preponderance of fibroblasts seen in microscopy of the cultures and thus would likely not effect molecular changes observed. Although cell culture experiments do not study the complex milieu that might be contributed by other cell populations (e.g. Myocytes or endothelial cells) specific to each chamber, the experiments performed in whole tissue (atria and ventricles) from mice do reflect changes in the entire milieu. Electrophysiology studies are reported using optical mapping in Langendorf perfused hearts. These experiments identify the electrophysiologic properties and substrate intrinsic to the heart, devoid of any autonomic or humoral effects. While the NP system may exert some effects via these mechanisms, these effects were not studied in this paper.

Supplementary material

Supplementary material is available at *Cardiovascular Research* online.

Acknowledgements

The NPR-C knockout mice were provided by Oliver Smithies (University of North Carolina). Thanks to Francisco Figueroa and Gregory Nah for helping with data analysis.

Conflict of interest: none declared.

Funding

This work was supported by the UCSF Naify Atrial Fibrillation Center.

References

1. Chugh SS, Blackshear JL, Shen WK, Hammill SC, Gersh BJ. Epidemiology and natural history of atrial fibrillation: clinical implications. *J Am Coll Cardiol* 2001;**37**:371–378.
2. Boldt A, Wetzel U, Lauschke J, Weigl J, Gummert J, Hindricks G, Kottkamp H, Dhein S. Fibrosis in left atrial tissue of patients with atrial fibrillation with and without underlying mitral valve disease. *Heart* 2004;**90**:400–405.
3. Marcus GM, Yang Y, Varosy PD, Ordovas K, Tseng ZH, Badhwar N, Lee BK, Lee RJ, Scheinman MM, Olgin JE. Regional left atrial voltage in patients with atrial fibrillation. *Heart Rhythm* 2007;**4**:138–144.
4. Nattel S. New ideas about atrial fibrillation 50 years on. *Nature* 2002;**415**:219–226.
5. Li D, Fareh S, Leung TK, Nattel S. Promotion of atrial fibrillation by heart failure in dogs: atrial remodeling of a different sort. *Circulation* 1999;**100**:87–95.
6. Lee KW, Everett TH, Rahmutula D, Guerra JM, Wilson E, Ding C, Olgin JE. Pirfenidone prevents the development of a vulnerable substrate for atrial fibrillation in a canine model of heart failure. *Circulation* 2006;**114**:1703–1712.
7. Kistler PM, Sanders P, Dodic M, Spence SJ, Samuel CS, Zhao C, Charles JA, Edwards GA, Kalman JM. Atrial electrical and structural abnormalities in an ovine model of chronic blood pressure elevation after prenatal corticosteroid exposure: implications for development of atrial fibrillation. *Eur Heart J* 2006;**27**:3045–3056.
8. Abed HS, Samuel CS, Lau DH, Kelly DJ, Royce SG, Alasady M, Mahajan R, Kuklik P, Zhang Y, Brooks AG, Nelson AJ, Worthley SG, Abhayaratna WP, Kalman JM, Wittert GA, Sanders P. Obesity results in progressive atrial structural and electrical remodeling: implications for atrial fibrillation. *Heart Rhythm* 2013;**10**:90–100.
9. Verheule S, Sato T, Everett Tt Engle SK, Otten D, Rubart-von der Lohe M. Increased vulnerability to atrial fibrillation in transgenic mice with selective atrial fibrosis caused by overexpression of TGF-beta1. *Circ Res* 2004;**94**:1458–1465.
10. Hanna N, Cardin S, Leung TK, Nattel S. Differences in atrial versus ventricular remodeling in dogs with ventricular tachypacing-induced congestive heart failure. *Cardiovasc Res* 2004;**63**:236–244.
11. Burstein B, Libby E, Calderone A, Nattel S. Differential behaviors of atrial versus ventricular fibroblasts: a potential role for platelet-derived growth factor in atrial-ventricular remodeling differences. *Circulation* 2008;**117**:1630–1641.
12. Nakajima H, Nakajima HO, Salcher O, Dittie AS, Dembowsky K, Jing S, Field LJ. Atrial but not ventricular fibrosis in mice expressing a mutant transforming growth factor-beta(1) transgene in the heart. *Circ Res* 2000;**86**:571–579.
13. Rahmutula D, Marcus GM, Wilson EE, Ding C-H, Xiao Y, Paquet AC, Barbeau R, Barczak AJ, Erle DJ, Olgin JE. Molecular basis of selective atrial fibrosis due to overexpression of transforming growth factor-β1. *Cardiovasc Res* 2013;**99**:769–779.
14. Shinagawa K, Shi YF, Tardif JC, Leung TK, Nattel S. Dynamic nature of atrial fibrillation substrate during development and reversal of heart failure in dogs. *Circulation* 2002;**105**:2672–2678.
15. Sanders P, Morton JB, Davidson NC, Spence SJ, Vohra JK, Sparks PB, Kalman JM. Electrical remodeling of the atria in congestive heart failure: electrophysiological and electroanatomic mapping in humans. *Circulation* 2003;**108**:1461–1468.
16. Nishikimi T, Maeda N, Matsuoka H. The role of natriuretic peptides in cardioprotection. *Cardiovasc Res* 2006;**69**:318–328.
17. Tamura N, Ogawa Y, Chusho H, Nakamura K, Nakao K, Suda M, Kasahara M, Hashimoto R, Katsuura G, Mukoyama M, Itoh H, Saito Y, Tanaka I, Otani H, Katsuki M. Cardiac fibrosis in mice lacking brain natriuretic peptide. *Proc Natl Acad Sci USA* 2000;**97**:4239–4244.
18. Li P, Wang D, Lucas J, Oparil S, Xing D, Cao X, Novak L, Renfrow MB, Chen Y-F. Atrial natriuretic peptide inhibits transforming growth factor beta-induced Smad signaling and myofibroblast transformation in mouse cardiac fibroblasts. *Circ Res* 2008;**102**:185–192.
19. Holtwick R, van Eickels M, Skryabin BV, Baba HA, Bubikat A, Begrow F, Schneider MD, Garbers DL, Kuhn M. Pressure-independent cardiac hypertrophy in mice with cardiomyocyte-restricted inactivation of the atrial natriuretic peptide receptor guanylyl cyclase-A. *J Clin Invest* 2003;**111**:1399–1407.
20. Tsuneyoshi H, Nishina T, Nomoto T, Kanemitsu H, Kawakami R, Unimonh O, Nishimura K, Komeda M. Atrial natriuretic peptide helps prevent late remodeling after left ventricular aneurysm repair. *Circulation* 2004;**110**:II174–II179.
21. Kapoun AM, Liang F, O'Young G, Damm DL, Quon D, White RT, Munson K, Lam A, Schreiner GF, Protter AA. B-type natriuretic peptide exerts broad functional opposition to transforming growth factor-beta in primary human cardiac fibroblasts: fibrosis, myofibroblast conversion, proliferation, and inflammation. *Circ Res* 2004;**94**:453–461.
22. Levin ER, Gardner DG, Samson WK. Natriuretic peptides. *N Engl J Med* 1998;**339**:321–328.
23. Lin X, Hanze J, Heese F, Sodmann R, Lang RE. Gene expression of natriuretic peptide receptors in myocardial cells. *Circ Res* 1995;**77**:750–758.
24. Cao L, Gardner DG. Natriuretic peptides inhibit DNA synthesis in cardiac fibroblasts. *Hypertension* 1995;**25**:227–234.
25. Matsukawa N, Grzesik WJ, Takahashi N, Pandey KN, Pang S, Yamauchi M, Smithies O. The natriuretic peptide clearance receptor locally modulates the physiological effects of the natriuretic peptide system. *Proc Natl Acad Sci USA* 1999;**96**:7403–7408.
26. Hu P, Zhang D, Swenson L, Chakrabarti G, Abel ED, Litwin SE. Minimally invasive aortic banding in mice: effects of altered cardiomyocyte insulin signaling during pressure overload. *Am J Physiol Heart Circ Physiol* 2003;**285**:H1261–H1269.
27. Martin TP, Robinson E, Harvey AP, MacDonald M, Grieve DJ, Paul A, Currie S. Surgical optimization and characterization of a minimally invasive aortic banding procedure to induce cardiac hypertrophy in mice. *Exp Physiol* 2012;**97**:822–832.
28. Gao S, Ho D, Vatner DE, Vatner SF. Echocardiography in mice. *Curr Protoc Mouse Biol* 2011;**1**:71–83.
29. Zhang H, Zhong H, Everett TH, Wilson E, Chang R, Zeng D, Belardinelli L, Olgin JE. Blockade of A2B adenosine receptor reduces left ventricular dysfunction and ventricular arrhythmias 1 week after myocardial infarction in the rat model. *Heart Rhythm* 2014;**11**:101–109.
30. Salama G, Kanai A, Efimov IR. Subthreshold stimulation of Purkinje fibers interrupts ventricular tachycardia in intact hearts. Experimental study with voltage-sensitive dyes and imaging techniques. *Circ Res* 1994;**74**:604–619.

31. Bayly PV, KenKnight BH, Rogers JM, Hillsley RE, Ideker RE, Smith WM. Estimation of conduction velocity vector fields from epicardial mapping data. *IEEE Trans Biomed Eng* 1998;**45**:563–571.
32. Lammers WJ, Schalij MJ, Kirchhof CJ, Allessie MA. Quantification of spatial inhomogeneity in conduction and initiation of reentrant atrial arrhythmias. *Am J Physiol* 1990; **259**:H1254–H1263.
33. Nishida K, Qi XY, Wakili R, Comtois P, Chartier D, Harada M, Iwasaki Y-K, Romeo P, Maguy A, Dobrev D, Michael G, Talajic M, Nattel S. Mechanisms of atrial tachyarrhythmias associated with coronary artery occlusion in a chronic canine model. *Circulation* 2011;**123**:137–146.
34. Winer J, Jung CK, Shackel I, Williams PM. Development and validation of real-time quantitative reverse transcriptase-polymerase chain reaction for monitoring gene expression in cardiac myocytes in vitro. *Anal Biochem* 1999;**270**:41–49.
35. Wang LW, Huttner IG, Santiago CF, Kesteven SH, Yu Z-Y, Feneley MP, Fatkin D. Standardized echocardiographic assessment of cardiac function in normal adult zebrafish and heart disease models. *Dis Model Mech* 2017;**10**:63–76.
36. Chang HY, Chi J-T, Dudoit S, Bondre C, van de Rijn M, Botstein D, Brown PO. Diversity, topographic differentiation, and positional memory in human fibroblasts. *Proc Natl Acad Sci USA* 2002;**99**:12877–12882.
37. Cha T-J, Ehrlich JR, Zhang L, Shi Y-F, Tardif J-C, Leung TK, Nattel S. Dissociation between ionic remodeling and ability to sustain atrial fibrillation during recovery from experimental congestive heart failure. *Circulation* 2004;**109**:412–418.
38. Ramos P, Rubies C, Torres M, Batlle M, Farre R, Brugada J, Montserrat JM, Almendros I, Mont L. Atrial fibrosis in a chronic murine model of obstructive sleep apnea: mechanisms and prevention by mesenchymal stem cells. *Respir Res* 2014;**15**:54.
39. Accornero F, van Berlo JH, Correll RN, Elrod JW, Sargent MA, York A, Rabinowitz JE, Leask A, Molkentin JD. Genetic analysis of connective tissue growth factor as an effector of transforming growth factor β signaling and cardiac remodeling. *Mol Cell Biol* 2015;**35**:2154–2164.
40. Rose RA, Giles WR. Natriuretic peptide C receptor signalling in the heart and vasculature. *J Physiol (Lond)* 2008;**586**:353–366.
41. Liao C-h, Akazawa H, Tamagawa M, Ito K, Yasuda N, Kudo Y, Yamamoto R, Ozasa Y, Fujimoto M, Wang P, Nakauchi H, Nakaya H, Komuro I. Cardiac mast cells cause atrial fibrillation through PDGF-A-mediated fibrosis in pressure-overloaded mouse hearts. *J Clin Invest* 2010;**120**:242–253.
42. Crozier I, Richards AM, Foy SG, Ikram H. Electrophysiological effects of atrial natriuretic peptide on the cardiac conduction system in man. *Pacing Clin Electrophysiol* 1993;**16**:738–742.
43. Stambler BS, Guo GB. Atrial natriuretic peptide has dose-dependent, autonomically mediated effects on atrial refractoriness and repolarization in anesthetized dogs. *J Cardiovasc Electrophysiol* 2005;**16**:1341–1347.
44. Yoshida T, Niwano S, Niwano H, Imaki R, Satoh D, Masaki Y, Nakazato K, Soma K, Izumi T. Atrial natriuretic peptide (ANP) suppresses acute atrial electrical remodeling in the canine rapid atrial stimulation model. *Int J Cardiol* 2008;**123**:147–154.
45. Núñez L, Vaquero M, Gómez R, Caballero R, Mateos-Cáceres P, Macaya C, Iriepa I, Gálvez E, López-Farré A, Tamargo J, Delpón E. Nitric oxide blocks hKv1.5 channels by S-nitrosylation and by a cyclic GMP-dependent mechanism. *Cardiovasc Res* 2006; **72**:80–89.
46. Egom EE, Vella K, Hua R, Jansen HJ, Moghtadaei M, Polina I, Bogachev O, Hurnik R, Mackasey M, Rafferty S, Ray G, Rose RA. Impaired sinoatrial node function and increased susceptibility to atrial fibrillation in mice lacking natriuretic peptide receptor C. *J Physiol* 2015;**593**:1127–1146.
47. Thomas SA, Schuessler RB, Berul CI, Beardslee MA, Beyer EC, Mendelsohn ME, Saffitz JE. Disparate effects of deficient expression of connexin43 on atrial and ventricular conduction: evidence for chamber-specific molecular determinants of conduction. *Circulation* 1998;**97**:686–691.
48. Friedrichs K, Adam M, Remane L, Mollenhauer M, Rudolph V, Rudolph TK, Andrié RP, Stöckigt F, Schrickel JW, Ravekes T, Deuschl F, Nickenig G, Willems S, Baldus S, Klinke A. Induction of atrial fibrillation by neutrophils critically depends on CD11b/CD18 integrins. *PLoS One* 2014;**9**:e89307.
49. Verheule S, van Batenburg CA, Coenjaerts FE, Kirchhofe S, Willecke K, Jongsma HJ. Cardiac conduction abnormalities in mice lacking the gap junction protein connexin40. *J Cardiovasc Electrophysiol* 1999;**10**:1380–1389.
50. Hussein AA, Saliba WI, Martin DO, Shadman M, Kanj M, Bhargava M, Dresing T, Chung M, Callahan T, Baranowski B, Tchou P, Lindsay BD, Natale A, Wazni OM. Plasma B-type natriuretic peptide levels and recurrent arrhythmia after successful ablation of lone atrial fibrillation. *Circulation* 2011;**123**:2077–2082.
51. Rossi A, Enriquez-Sarano M, Burnett JC Jr, Lerman A, Abel MD, Seward JB. Natriuretic peptide levels in atrial fibrillation: a prospective hormonal and Doppler-echocardiographic study. *J Am Coll Cardiol* 2000;**35**:1256–1262.
52. Seegers J, Zabel M, Grüter T, Ammermann A, Weber-Krüger M, Edelmann F, Gelbrich G, Binder L, Herrmann-Lingen C, Gröschel K, Hasenfuß G, Feltgen N, Pieske B, Wachter R. Natriuretic peptides for the detection of paroxysmal atrial fibrillation. *Open Heart* 2015;**2**:e000182.
53. van den Berg MP, van Gelder IC, van Veldhuisen DJ. Depletion of atrial natriuretic peptide during longstanding atrial fibrillation. *Europace* 2004;**6**:433–437.
54. Hodgson-Zingman DM, Karst ML, Zingman LV, Heublein DM, Darbar D, Herron KJ, Ballew JD, de Andrade M, Burnett JC, Olson TM. Atrial natriuretic peptide frameshift mutation in familial atrial fibrillation. *N Engl J Med* 2008;**359**:158–165.
55. Hua R, MacLeod SL, Polina I, Moghtadaei M, Jansen HJ, Bogachev O, O'Blenes SB, Sapp JL, Legare J-F, Rose RA. Effects of wild-type and mutant forms of atrial natriuretic peptide on atrial electrophysiology and arrhythmogenesis. *Circ Arrhythm Electrophysiol* 2015;**8**:1240–1254.
56. Ren X, Xu C, Zhan C, Yang Y, Shi L, Wang F, Wang C, Xia Y, Yang B, Wu G, Wang P, Li X, Wang D, Xiong X, Liu J, Liu Y, Liu M, Liu J, Tu X, Wang QK. Identification of NPPA variants associated with atrial fibrillation in a Chinese GeneID population. *Clin Chim Acta* 2010;**411**:481–485.
57. Li Y, Kishimoto I, Saito Y, Harada M, Kuwahara K, Izumi T, Takahashi N, Kawakami R, Tanimoto K, Nakagawa Y, Nakanishi M, Adachi Y, Garbers DL, Fukamizu A, Nakao K. Guanylyl cyclase-A inhibits angiotensin II type 1A receptor-mediated cardiac remodeling, an endogenous protective mechanism in the heart. *Circulation* 2002;**106**:1722–1728.
58. Fujisaki H, Ito H, Hirata Y, Tanaka M, Hata M, Lin M, Adachi S, Akimoto H, Marumo F, Hiroe M. Natriuretic peptides inhibit angiotensin II-induced proliferation of rat cardiac fibroblasts by blocking endothelin-1 gene expression. *J Clin Invest* 1995;**96**:1059–1065.
59. Bujak M, Frangogiannis NG. The role of TGF-beta signaling in myocardial infarction and cardiac remodeling. *Cardiovasc Res* 2007;**74**:184–195.
60. Kato J, Lanier-Smith KL, Currie MG. Cyclic GMP down-regulates atrial natriuretic peptide receptors on cultured vascular endothelial cells. *J Biol Chem* 1991;**266**: 14681–14685.
61. Kato J, Misko TP, Currie MG. Induction of nitric oxide synthase regulates atrial natriuretic peptide receptors in vascular smooth muscle cells. *Eur J Pharmacol* 1993;**244**: 153–159.
62. Kim AM, Olgin JE, Everett TH. Role of atrial substrate and spatiotemporal organization in atrial fibrillation. *Heart Rhythm* 2009;**6**:S1–S7.